ISSN 1070-3284, Russian Journal of Coordination Chemistry, 2024, Vol. 50, No. 5, pp. 307–315. © Pleiades Publishing, Ltd., 2024.

Monomeric and Polymeric Cyclopentadienyl Dysprosium Complexes Based on the Acenaphthene-1,2-diimine Ligand

D. A. Lukina[a], A. A. Skatova[a], E. A. Kozlova[a], and I. L. Fedushkin[a, *]

[a] *Razuvaev Institute of Organometallic Chemistry, Russian Academy of Sciences, Nizhny Novgorod, Russia*

**e-mail: igorfed@iomc.ras.ru*

Received November 14, 2023; revised February 8, 2024; accepted February 8, 2024

Abstract—The reaction of [(Dpp-bian)DyI(Dme)$_2$] (Dpp-bian is 1,2-bis[(2,6-diisopropylphenyl)imino]acenaphthene, Dme is $CH_3OCH_2CH_2OCH_3$) with Cp*K (Cp* is C_5Me_5) in toluene followed by crystallization from benzene affords crystals of the 1D coordination polymer [(Dpp-bian)DyIKCp*]$_n$ (**I**)·2.6C_6H_6 (26%) and crystals of the monomeric complex [(Dpp-bian)DyCp*(Dme)] (**II**)·1.5C_6H_6 (12%). The same reaction in 1,2-dimethoxyethane followed by crystallization from benzene makes it possible to isolate only complex **II**·1.5C_6H_6 in a yield of 48%. The synthesized compounds are characterized by IR and UV spectroscopy and elemental and thermogravimetric analyses. Their molecular structures are determined by XRD (CIF files CCDC nos. 2298407 (**I**) and 2298408 (**II**)).

Keywords: dysprosium, cyclopentadienyl, 1,2-bis(arylimino)acenaphthene, coordination polymer, redox-active ligand

DOI: 10.1134/S1070328424600207

INTRODUCTION

Metal-organic frameworks (MOFs) attract increasing attention of researchers due to a high porosity and a broad range of practical application [1], including gas storage [2], separation of complicated mixtures [3, 4], and catalysis [5]. In particular, they became objects of active investigation owing to the use as components of fuel cells and supercapacitors [1]. The presence of magnetic or photoactive centers (e.g., *d*- or *f*-element cations, organic radical ligands) in polymeric molecules of MOFs [6] makes it possible to prepare molecular magnets [7] and related photomagnets and photoactive materials [8–10], which can be used for the fabrication of information carriers of new types, quantum computers, and diverse magnetic and optical mechanical devices.

Since the structures of MOFs and their properties depend on the oxidation state of the metal and reduction state of the ligands, the presence of redox-active sites provides a possibility of fabricating MOFs with switchable properties [11–14]. In this context, we are interested in the ligand that can donate or accept electrons upon the coordination of the metal center within the MOF structure. 1,2-Bis(arylimino)acenaphthenes have a rigid structure and can act as both electron and proton sponges. 1,2-Bis[(2,6-diisopropylphenyl)imino]acenaphthene (Dpp-bian) is the most widely used ligand of this family and can act as an electron reservoir to form the radical anion or dianion upon reduction by metals of groups 1 [15], 2 [16], and 13 [17, 18] and by lanthanides [19–22]. In the case of alkaline metals and lanthanides, the compounds with Dpp-bian tri- and tetraanions can be formed [15, 23–25]. In the chemistry of rare-earth elements, Ar-bian ligands make it possible to form structurally unusual molecular systems demonstrating interesting spectral, magnetic, and chemical properties. The complexes of divalent ytterbium, samarium, and europium with the bulky ligands Ar^{BIG}-bian, [(Ar^{BIG}-bian)Yb(Dme)], [(Ar^{BIG}-bian)Sm], and [(Ar^{BIG}-bian)Eu(Thf)$_2$] (Ar^{BIG}-bian is 1,2-bis[(2,6-dibenzhydryl-4-methylphenyl)imino]acenaphthene) have recently been synthesized [26, 27]. The absence (restricted presence) of solvent molecules in the coordination sphere of metal atoms in these compounds compels metal cations to "coordinate" phenyl rings. This interaction is mainly electrostatic in character and is reduced to the interaction of the cation with π systems of the phenyl rings. We pioneered in accomplishing the thermally induced metal–ligand electron transfer (valence tautomerism) in the complex of the rare-earth element, namely, ytterbium complex [(Dpp-bian)Yb(μ-Cl)(Dme)]$_2$ [28]. The 1D coordination polymer [(Dpp-bian)-Eu(4,4-Bipy)(Thf)$_2$·4(Thf)]$_n$ [29] bearing 4,4-bipyridyl (4,4-Bipy) as the linker was synthesized from redox-active Dpp-bian. The elementary unit of the coordination polymer contains three paramagnetic centers: (Dpp-bian)$^{\bullet-}$ (S = 1/2), (4,4'-Bipy)$^{\bullet-}$ (S = 1/2), and Eu^{2+} (S = 7/2). Their magnetic ordering occurs at low temperatures. The study of the field

dependence of the magnetization shows that the europium polymer is metamagnetic at temperatures below 4 K. The 1D coordination polymers containing lanthanides with cyclopentadienyl ligands as linkers are also known [30–34]. The reactions of Cp*K (Cp* is C_5Me_5) with the lanthanum [(Dpp-bian)LaI(Thf)$_2$]$_2$ [24] and samarium [(Ar^{BIG}-bian)SmI(Dme)] [35] complexes in solvating solvents were shown to afford the corresponding monomeric complexes [(Dpp-bian)LaICp*][Na(18-crown-6)(Thf)$_2$], [(Dpp-bian)-LaCp*(Thf)] [24], and [(Ar^{BIG}-bian)SmICp*]-[K(Dme)$_4$] [35]. Thus, the preparation of the coordination polymers from the lanthanide complexes bearing cyclopentadienyl and redox-active ligands is an urgent task.

In this work, we report the syntheses of the dysprosium complexes [(Dpp-bian)DyIKCp*]$_n$ (**I**) and [(Dpp-bian)DyCp*(Dme)] (**II**) and the results of studying their structures.

EXPERIMENTAL

Compounds **I** and **II** are sensitive to air oxygen and moisture and, hence, all manipulations on their synthesis, isolation, and identification were carried out in vacuo using the Schlenk technique or in argon (Glovebox M. Braun). Ligand Dpp-bian was synthesized using a known procedure [36]. 1,2-Dimethoxyethane (DME), toluene, and benzene were dehydrated over the sodium complex with benzophenone ketyl and sampled by condensation in vacuo prior to use. IR spectra were recorded on an FSM-1201 spectrometer. Samples of the compounds were prepared in an inert atmosphere of argon as suspensions in Nujol. Elemental analysis was conducted by burning the samples in an Elementar Vario EL Cube automated analyzer. The yields of products **I** and **II** were based on the initial amount of Dpp-bian. UV spectra were detected on Termo Evolution 201 and Perkin-Elmer λ 25 spectrometers. Thermogravimetric analysis (TG) was carried out on a TGA/DSC 3+ METTLER TOLEDO instrument in a temperature range of 40–400°C in a nitrogen flow at a flow rate of 50 mL min^{-1}, a heating rate of 5°C min^{-1}, and weighting samples of 15.858 and 9.034 mg for compounds **I** and **II**, respectively.

Synthesis of [(Dpp-bian)DyIKCp*]$_n$ (I)·2.6C$_6$H$_6$. Diiodine I_2 (0.064 g, 0.25 mmol) and Dpp-bian (0.25 g, 0.5 mmol) were added to a metallic dysprosium excess (30 g, 185 mmol) in DME (30 mL). The mixture was heated at 100°C for 3 h. The solution color changed from orange to blue. The resulting solution was separated by filtration, and the solvent was changed by toluene (15 mL). The toluene solution was added with Cp*K (0.09 g, 0.5 mmol). The reaction mixture was heated for 30 min until the solution turned green. A colorless precipitate of potassium iodide was separated by centrifugation, the solvent was removed in vacuo, and the residue was dissolved in benzene (4 mL). Green crystals of compound **I**·2.6C$_6$H$_6$ suitable for XRD were isolated from the solution. The yield was 0.15 g (26%).

For $C_{61.53}H_{72.75}N_2IKDy$ (FW = 1168.84)

Anal. calcd., %	C, 63.22	H, 6.27	N, 2.39
Found, %	C, 63.07	H, 6.12	N, 2.23

IR (Nujol; ν, cm^{-1}): 1609 w, 1578 m, 1306 s, 1250 m, 1221 w, 1208 w, 1188 w, 1159 w, 1103 m, 1055 w, 1036 m, 1003 w, 933 w, 916 m, 887 w, 872 w, 822 m, 800 m, 777 m, 762 m, 675 s, 623 m, 596 w, 547 w, 513 w, 491 w.

The subsequent crystallization from a concentrated mother liquor (1 mL) gave dark, almost black crystals of the complex [(Dpp-bian)DyCp*(Dme)] (**II**)·1.5C$_6$H$_6$ suitable for XRD in a yield of 12% (0.06 g).

Synthesis of [(Dpp-bian)DyCp*(Dme)] (II)·1.5C$_6$H$_6$. Iodine I_2 (0.064 g, 0.25 mmol) and Dpp-bian (0.25 g, 0.5 mmol) were added to a metallic dysprosium excess (30 g, 185 mmol) in DME (30 mL). The mixture was heated at 100°C for 3 h. The solution color changed from orange to blue. A blue solution filtered from a metal excess was added with Cp*K (0.09 g, 0.5 mmol). The solution turned green. The solvent was removed in vacuo, the residue was dissolved in benzene (5 mL), and the solution was separated from a potassium iodide precipitate by centrifugation and decantation. Dark crystals of complex **II**·1.5C$_6$H$_6$ suitable for XRD were isolated from the concentrated solution (2 mL) in a yield of 0.24 g (48%).

For $C_{59}H_{74}N_2O_2Dy$ (FW = 1005.70)

Anal. calcd., %	C, 70.46	H, 7.42	N, 2.78
Found, %	C, 70.37	H, 7.18	N, 2.51

IR (Nujol; ν, cm^{-1}): 1612 w, 1580 m, 1430 s, 1300 s, 1252 m, 1219 w, 1208 w, 1190 w, 1159 w, 1126 m, 1099 m, 1049 m, 1028 m, 1003 w, 953 m, 932 w, 916 m, 889 w, 870 w, 852 m, 818 m, 806 m, 800 w, 771 m, 764 s, 675 s, 623 m, 640 w, 511 w, 493 w.

XRD of the synthesized compounds was carried out on an Oxford Xcalibur Eos diffractometer (graphite monochromator, MoK_α radiation, ω scan mode, λ = 0.71073 Å). Experimental sets of intensities were integrated using the CrysAlisPro program [37]. Absorption corrections were applied using the SCALE3 ABSPACK scaling algorithm implemented in the CrysAlisPro program. The structures were solved using the SHELXT program [38] and refined by full-matrix least squares for F^2_{hkl} in the anisotropic approximation for all non-hydrogen atoms using the SHELXL program [39]. Hydrogen atoms were placed in the geometrically calculated positions and refined

Table 1. Crystallographic data and XRD parameters for compounds **I**·2.6C_6H_6 and **II**·1.5C_6H_6

Parameter	Value	
	I·2.6C_6H_6	**II**·1.5C_6H_6
Empirical formula	$C_{61.53}H_{72.75}N_2IKDy$	$C_{59}H_{74}N_2O_2Dy$
FW	1168.84	1005.7
Temperature	298(2)	298(2)
Crystal system	Orthorhombic	Triclinic
Space group	*Fdd*2	$P\bar{1}$
a, Å	31.8240(14)	11.9242(2)
b, Å	30.0889(10)	12.7222(2)
c, Å	21.9899(8)	17.5679(4)
α, deg	90	89.2338(16)
β, deg	90	89.5520(17)
γ, deg	90	82.1441(16)
V, Å^3	21056.4(14)	4321.54(12)
Z	16	2
ρ_{calc}, g/cm^3	1.475	1.265
μ, cm^{-1}	2.126	1.457
F(000)	9503	1048
Crystal sizes	0.45 × 0.19 × 0.19	0.79 × 0.62 × 0.36
Data collection range over θ, deg	2.252–25.350	2.083–25.681
Number of reflections: measured/independent	39664/9636	23645/9919
R_{int}	0.0488	0.0272
R_1, wR_2 (all reflections)	0.0492, 0.0931	0.0426, 0.0933
R_1, wR_2 ($I > 2\sigma(I)$)	0.0383, 0.0867	0.0361, 0.0903
$S(F^2)$	1.01	1.065
$\Delta\rho_{min}/\Delta\rho_{max}$, e/Å^3	0.669/–0.491	0.712/–0.790

in the isotropic approximation using the riding model: $U_{iso}(H) = 1.5\ U_{eq}(C)$ for methyl groups, and $U_{iso}(H) = 1.2\ U_{eq}(C)$ for all other groups.

In complex **I**, the isopropyl and aryl fragments are disordered over two positions. The RIGU, EADP, and DFIX instructions were used to restraint the geometric characteristics and anisotropic parameters of atomic shifts when refining the disordered fragments. The contribution of the solvent molecules to the overall X-ray radiation scattering of complex **I** was taken into account using the SQUEEZE program [40]. About 2.6 benzene molecules fall onto each molecule of the complex. In complex **II**, the benzene molecules and fragment of coordinated DME are disordered over two positions. The RIGU, EADP, DFIX, and ISOR instructions were used to restraint the geometric characteristics and anisotropic parameters of atomic shifts when refining the disordered fragments. The main crystallographic characteristics of complexes **I** and **II** are listed in Table 1. Selected bond lengths and bond angles are given in Table 2.

The structures were deposited with the Cambridge Crystallographic Data Centre (CIF files CCDC nos. 2298407 (**I**) and 2298408 (**II**); http://www.ccdc.cam.ac.uk).

RESULTS AND DISCUSSION

The reaction of equimolar amounts of [(Dppbian)DyI(Dme)$_2$] [41] and Cp*K (Cp* is C_5Me_5) (Scheme 1) in toluene on reflux for 30 min results in a change of the solution color from blue to green. Crystallization from benzene gave compounds [(Dppbian)DyIKCp*]$_n$ (**I**)·2.6C_6H_6 (26%) and [(Dppbian)DyCp*(Dme)] (**II**)·1.5C_6H_6 (12%) as dark crystals.

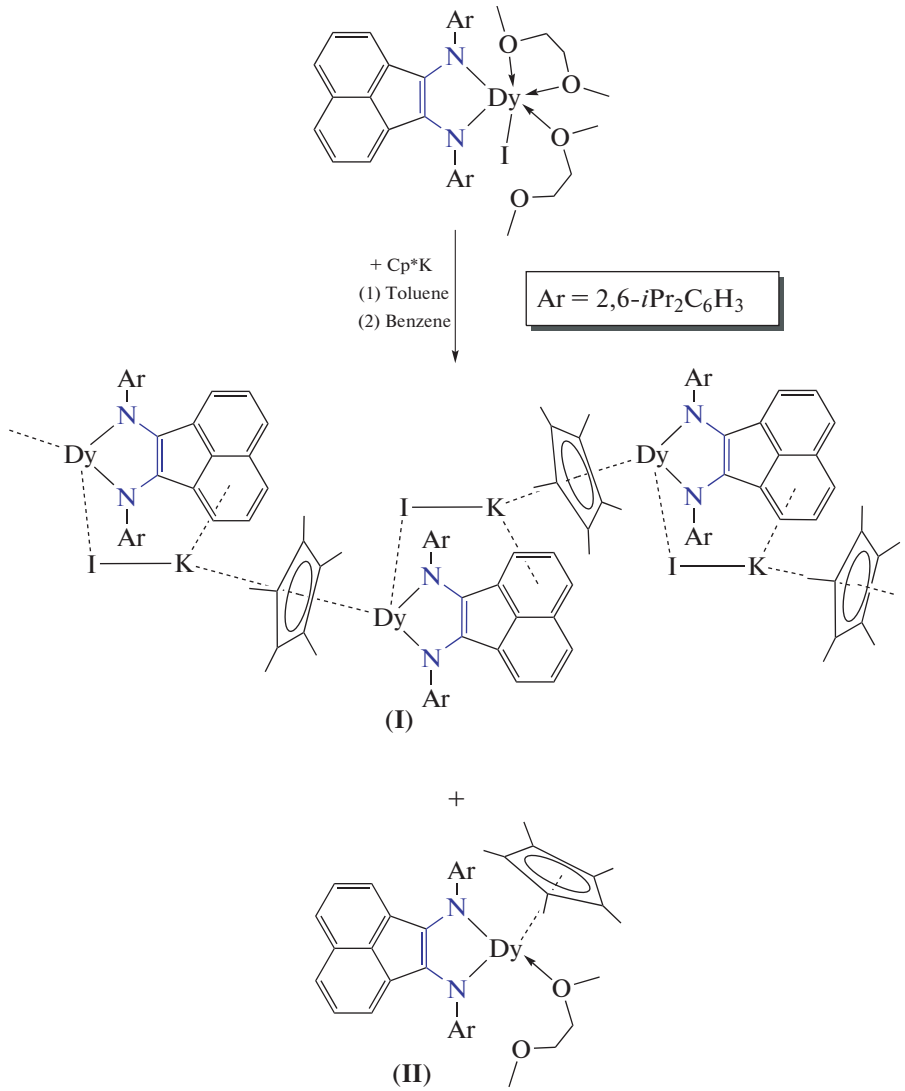

Scheme 1.

Compound **I** contains no coordinated solvent and, hence, has a polymeric structure. On the contrary, in compound **II**, the dysprosium atom coordinates one DME molecule favoring the formation of the monomeric complex. To prove the formation of the monomeric structure of complex **II** by the presence of DME molecules in the coordination sphere of dysprosium, the reaction of equimolar amounts of the initial compound [(Dpp-bian)DyI(Dme)$_2$] and Cp*K in coordinating DME was conducted. The solution color changed from blue to green during the reaction, and the subsequent crystallization from benzene results in the formation of crystals of complex **II** in a yield of 48%. The composition and structure of the complex were confirmed by IR spectroscopy and XRD. The band of stretching vibrations of the C–N ordinary bond in the IR spectra of complexes **I** and **II** (1306 and 1300 cm^{-1}, respectively) confirms the dianionic state of the Dpp-bian ligand. UV spectroscopy is a universal tool for the determination of the reduction state of Dpp-bian in the metal complexes in solutions, since the absorption maxima of (Dpp-bian)^0, (Dpp-bian)$^-$, and (Dpp-bian)$^{2-}$ differ substantially [42]. Owing to the polymeric nature, compound **I** is poorly soluble in benzene: a slightly green-colored solution is formed upon dissolution, and its spectrum exhibits transmission and absorption maxima at 513 and 733 nm, respectively (Fig. 1). The spectrum of compound **II** in benzene has an absorption maximum at 606 nm (blue color, transmission maximum at 465 nm) (Fig. 1), which is characteristic of the lanthanide(III) complexes with the dianionic acenaphthene-1,2-diimine ligand Dpp-bian. For instance, the absorption maximum in the spectrum of a solution of the [(Dpp-bian)Sm(μ-Br)(Dme)]$_2$ complex in THF is observed at 640 nm [20], and that of the ytterbium compound

[(Dpp-bian)Yb[SC(S)NMe$_2$](Dme)] in DME lies at 691 nm [43]. The molar absorption coefficients could not reliably be determined because of a high sensitivity of compounds **I** and **II** to oxygen and moisture.

The TG data for product **I** demonstrates a smooth mass loss curve (Fig. 2a). The coordination polymer decomposed gradually on heating at 40–345°C. The TG data for compound **II** shows two mass loss stages (Fig. 2b). At the first stage (133–162°C, V_{max} at 146°C), the solvent molecules are liberated from the crystalline lattice. The complete destruction of the complex occurs at the next stage (162–338°C, V_{max} at 306°C). It is difficult to quantitatively estimate the mass loss in both compounds, since the stages are superimposed.

According to the XRD data, compound **I** represents 1D MOF (Fig. 3) and consists of infinite one-dimensional zigzag chains. Polymer assembling occurs due to binding one {(Dpp-bian)Dy} fragment simultaneously with the pentamethylcyclopentadienyl ligand and ion pair KI, which act as linkers. In compound **I**, the Dpp-bian ligand exists in the dianionic state, which is confirmed by the bond lengths in the diimine fragment N(1)C(1)C(2)N(2): N(1)–C(1) 1.401(10), N(2)–C(2) 1.376(11), and C(1)–C(2) 1.417(13) Å (Table 2). For example, in the lanthanide complexes with the Dpp-bian dianions, the mentioned bond lengths are 1.407(6), 1.391(6), and 1.418(6) Å, respectively, for [(Dpp-bian)LaCp*(Thf)] [24], and for [(Dpp-bian)SmBr(Dme)]$_2$ they are 1.403(3), 1.397(3), and 1.384(3) Å [20]. The Dy–N distances (2.187(7) and 2.214(7) Å) indicate the presence of the Dy^{3+} ion in product **I** [44]. The five-membered metallocycle in compound **I** is not planar, and the dihedral angle between the NCCN and NDyN planes is 138.2°. The distances between the dysprosium atom and carbon atoms of the cyclopentadienyl ligand lie in a narrow range (2.637(9)–2.676(9) Å), which indicates the η^5 coordination of the latter. The Dy–Cp$_{centr}$ distance (2.375 Å) is shorter than that in the samarium complex [(Ar^{BIG}-bian)SmICp*]-[K(Dme)$_4$] (2.430 Å) [35] and lanthanum compounds [(Dpp-bian)LaICp*][Na(18-crown-6)(Thf)$_2$] and [(Dpp-bian)LaCp*(Thf)] (2.535 and 2.505 Å, respectively) [24]. The observed dependence reflects a decrease in the ion radius of the central atom on going from lanthanum to samarium and further to dysprosium. In tris(pentamethylcyclopentadienyl)dysprosium [Cp$^*_3$Dy], the Dy–Cp$_{centr}$ distance is slightly longer than that in compound **I** and the Dy–C(Cp) distances range from 2.505 to 2.544 Å [45].

The molecular chains in the crystals of compound **I** are nearly perpendicular to each other (Fig. 4) and form cavities occupied by the solvent molecules.

Table 2. Selected bond lengths and angles in compounds **I**·2.6C$_6$H$_6$ and **II**·1.5C$_6$H$_6$

Bond	**I**	**II**
	d, Å	
C(1)–C(2)	1.417(13)	1.404(5)
N(1)–C(1)	1.401(10)	1.391(4)
N(2)–C(2)	1.376(11)	1.396(5)
Dy–N(1)	2.187(7)	2.214(3)
Dy–N(2)	2.214(7)	2.207(3)
Dy–I	3.0026(7)	
K–I	3.450(3)	
Dy–Cp$^*_{centr}$	2.375	2.358
K–Cp$^*_{centr}$	2.787	
Angle	ω, deg	
N(1)Dy–(2)	59.5(3)	58.54(11)
N(1)DyN(2)	84.2(3)	83.11(12)
DyIK	92.49(5)	

Unlike polymer **I**, complex **II** is monomeric (Fig. 5). Owing to the filling of the coordination sphere of the dysprosium atom by the DME molecule, the molecule of complex **II** contains no potassium iodide. The dysprosium atom coordinates the diimine and pentamethylcyclopentadienyl ligands, as well as

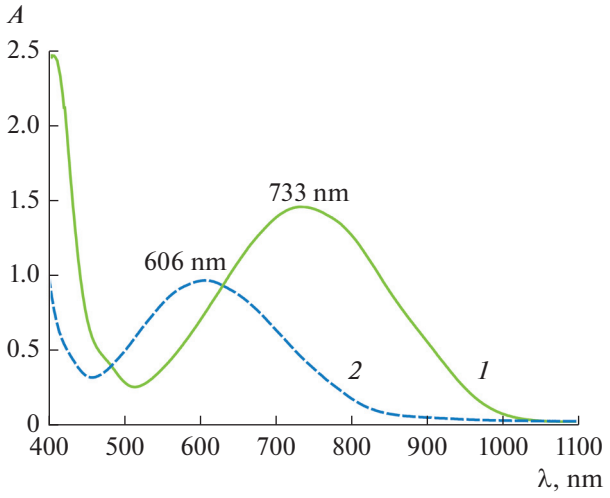

Fig. 1. Electronic absorption spectra of complexes (*1*) **I** and (*2*) **II** in benzene.

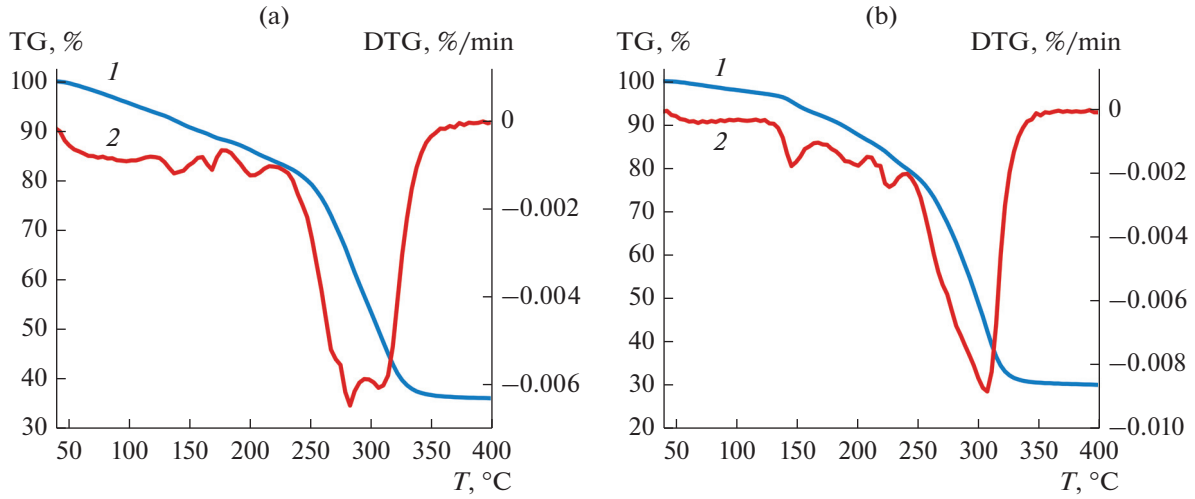

Fig. 2. Thermogravimetric analysis of complexes (a) **I** and (b) **II**: (*1*) TG and (*2*) DTG.

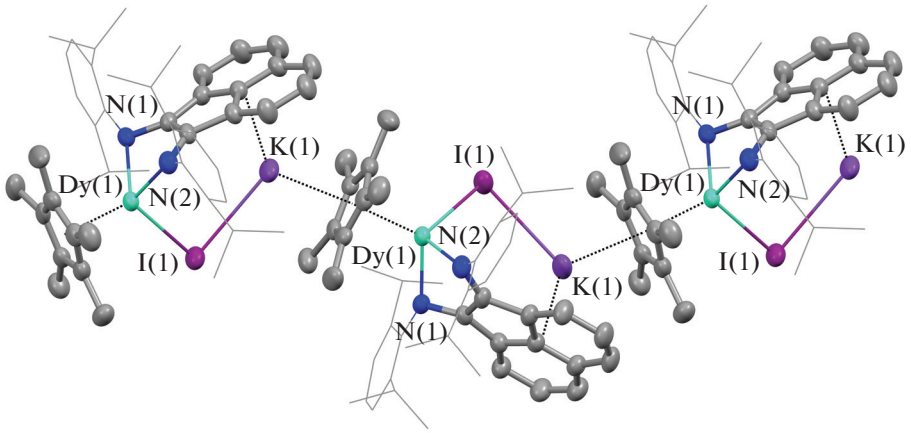

Fig. 3. Fragment of the molecular structure of 1D coordination polymer **I**. Hydrogen atoms are omitted.

the DME molecule, which is bound via the monodentate mode. Three benzene molecules fall onto two molecules of the complex in the crystal. The bond lengths N(1)–C(1), N(2)–C(2), and C(1)–C(2) (1.391(4), 1.396(5), and 1.404(5) Å, respectively) in the diimine fragment are consistent with the values for the same bonds in product **I**, which confirms the dianionic state of the ligand in both cases. The Dy–N distances (2.207(3) and 2.214(3) Å) in complex **II** are similar to the Dy–N distances in polymer **I**. The five-membered metallocycle in complex **II** is not planar, and the dihedral angle between the NCCN and NDyN planes is 138.4°, which is close to the value of the corresponding angle in product **I** (138.2°). The Dy–Cp_{centr} distance is 2.358 Å (for comparison, this distance in polymer **I** is 2.375 Å).

The molecules of complex **II** in the crystal are arranged in pairs oriented to each other by the cyclopentadienyl ligands lying in parallel planes (Fig. 6). As far as we know, such mutual arrangement of neutral molecules was never observed. The distance between the centers of the cyclopentadienyl rings (4.09 Å) exceeds the geometric criterion for the intermolecular π...π stacking [46], most likely, due to the electrostatic repulsion of the cyclopentadienyl rings.

Thus, we showed that the reaction of the dysprosium iodide complex [(Dpp-bian)DyI$(Dme)_2$] with Cp*K afforded compounds with different structures depending on the solvent nature: the predominantly solvate-free 1D coordination polymer of dysprosium based on the Dpp-bian ligand [(Dpp-bian)-DyIKCp*]$_n$ (**I**) is formed in nonsolvating toluene, and

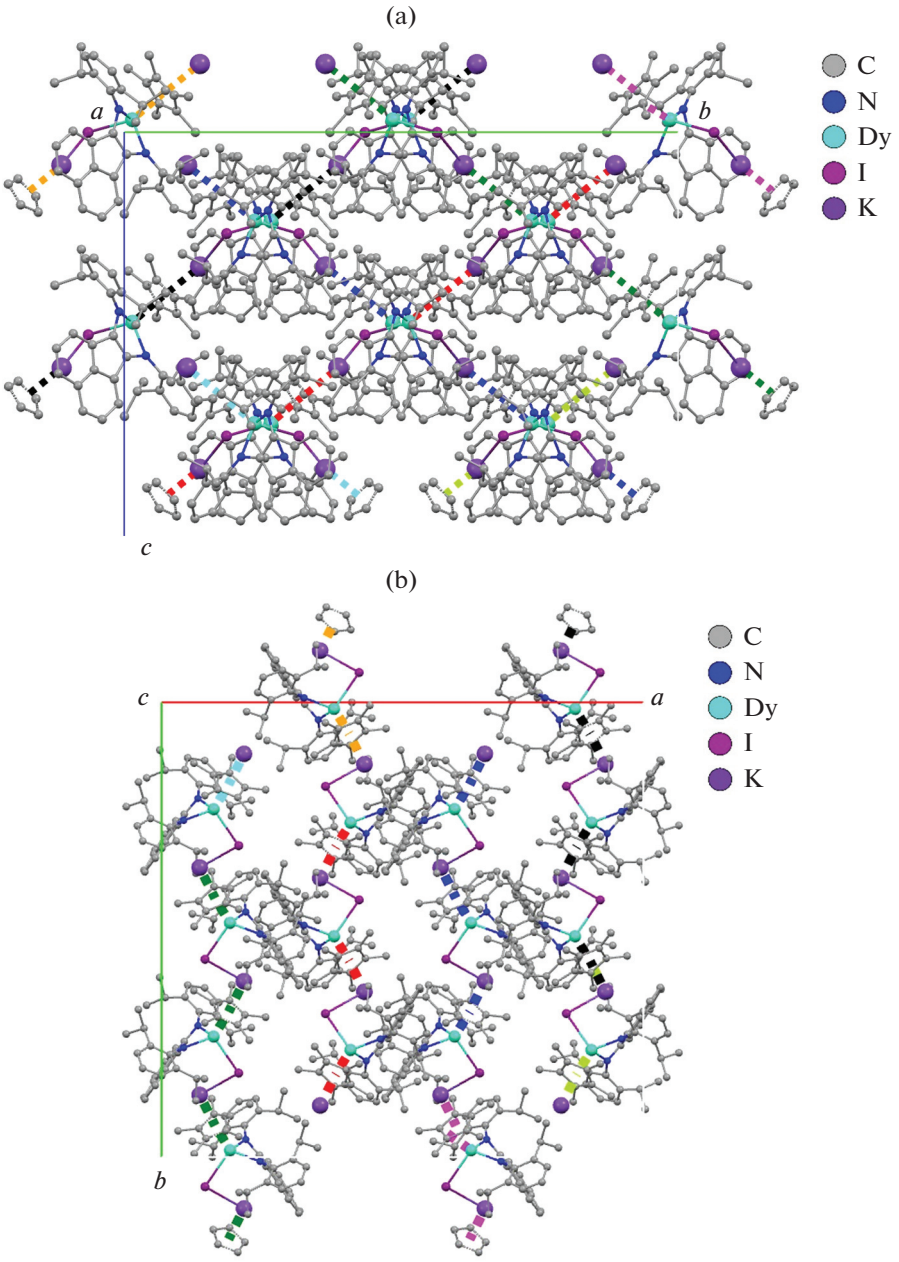

Fig. 4. Fragment of the crystal packing of complex **I**. The crystallographic projections along the (a) *a* axis and (b) *c* axis are presented. Hydrogen atoms and solvent molecules are omitted.

the monomeric complex [(Dpp-bian)DyCp*(Dme)] (**II**) containing one molecule of monodentate-bound DME is formed in solvating DME. Both the potassium iodide molecule and pentamethylcyclopentadienyl ligand are linking units in the assembling of polymer **I**. The unusual interaction of the pentamethylcyclopentadienyl rings in the crystal of complex **II** requires detailed studying by spectral and calculation methods, which will be performed in the nearest future.

ACKNOWLEDGMENTS

The work was carried out using the equipment of the Center for Collective Use "Analytical Center of Institute of Organometallic Chemistry of Russian Academy of Sciences."

FUNDING

This work was supported by the Russian Science Foundation, project no. 19-13-00336-П.

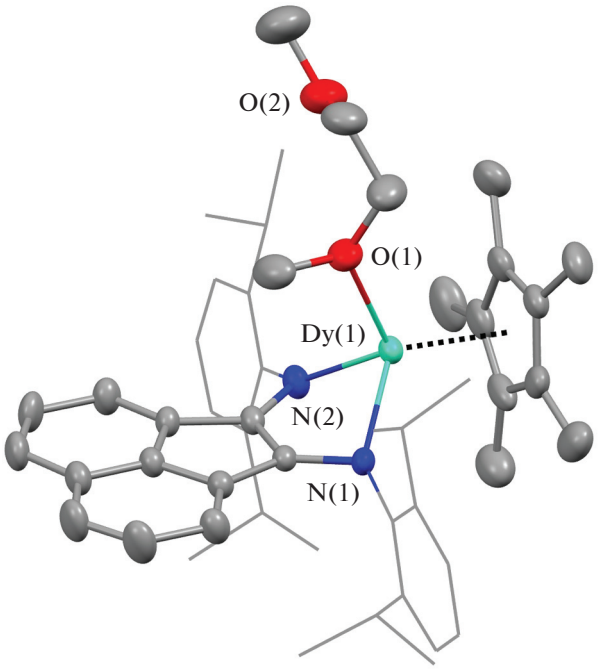

Fig. 5. Molecular structure of complex **II**. Hydrogen atoms are omitted.

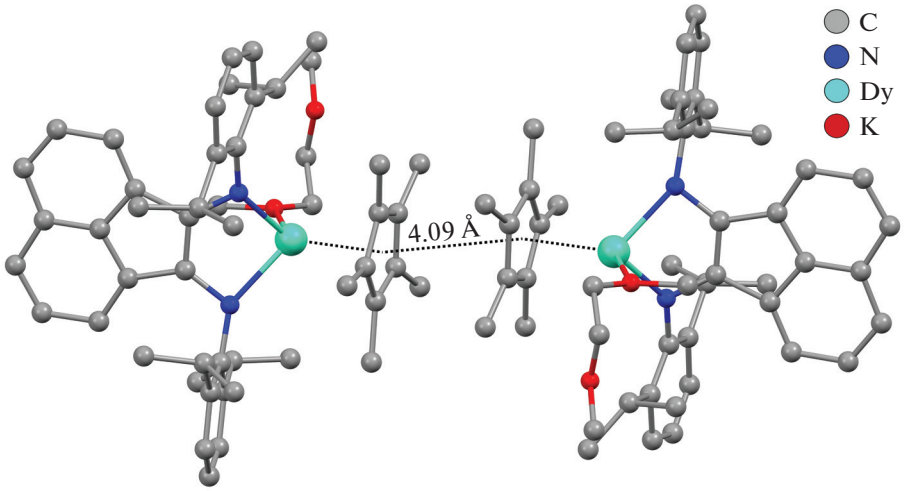

Fig. 6. Formation of pairs of molecules of complex **II** in the crystal. Hydrogen atoms are omitted.

CONFLICT OF INTEREST

The authors of this work declare that they have no conflicts of interest.

REFERENCES

1. Furukawa, H., Cordova, K.E., O'Keeffe, M., et al., *Science*, 2013, vol. 341, no. 6149, p. 1230444.
2. Lin, R.-B., Xiang, S., Zhou, W., et al., *Chem.*, 2020, vol. 6, no. 2, p. 337.
3. Li, J.-R., Kuppler, R.J., and Zhou, H.-C., *Chem. Soc. Rev.*, 2009, vol. 38, no. 5, p. 1477.
4. Li, J.-R., Sculley, J., and Zhou, H.-C., *Chem. Rev.*, 2012, vol. 112, no. 2, p. 869.
5. Lee, J., Farha, O.K., Roberts, J., et al., *Chem. Soc. Rev.*, 2009, vol. 38, no. 5, p. 1450.
6. Agafonov, M.A., Alexandrov, E.V., Artyukhova, N.A., et al., *J. Struct. Chem.*, 2022, vol. 63, p. 671.
7. Kurmoo, M., *Chem. Soc. Rev.*, 2009, vol. 38, no. 5, p. 1353.
8. Lustig, W.P., Mukherjee, S., Rudd, N.D., et al., *Chem. Soc. Rev.*, 2017, vol. 46, no. 11, p. 3242.
9. Cui, Y., Yue, Y., Qian, G., et al., *Chem. Rev.*, 2012, vol. 112, no. 2, p. 1126.

10. Rocha, J., Carlos, L.D., Paz, F.A.A., et al., *Chem. Soc. Rev.*, 2011, vol. 40, no. 2, p. 926.
11. Bazyakina, N.L., Makarov, V.M., Ketkov, S.Yu., et al., *Inorg. Chem.*, 2021, vol. 60, no. 5, p. 3238.
12. D'Alessandro, D.M., *Chem. Commun.*, 2016, vol. 52, no. 58, p. 8957.
13. Calbo, J., Golomb, M.J., and Walsh, A., *J. Mater. Chem. A*, 2019, vol. 7, no. 28, p. 16571.
14. Kharitonov, A.D., Trofimova, O.Y., Meshcheryakova, I.N., et al., *CrystEngComm*, 2020, vol. 22, no. 28, p. 4675.
15. Fedushkin, I.L., Skatova, A.A., Chudakova, V.A., et al., *Angew. Chem., Int. Ed. Engl.*, 2003, vol. 42, no. 28, p. 3294.
16. Fedushkin, I.L., Skatova, A.A., Chudakova, V.A., et al., *Eur. J. Inorg. Chem.*, 2003, vol. 2003, no. 18, p. 3336.
17. Lukoyanov, A.N., Fedushkin, I.L., Hummert, M., et al., *Russ. Chem. Bull.*, 2006, vol. 55, p. 422.
18. Fedushkin, I.L., Lukoyanov, A.N., Tishkina, A.N., et al., *Chem.-Eur. J.*, 2010, vol. 16, no. 25, p. 7563.
19. Fedushkin, I.L., Maslova, O.V., Baranov, E.V., et al., *Inorg. Chem.*, 2009, vol. 48, no. 6, p. 2355.
20. Fedushkin, I.L., Maslova, O.V., Hummert, M., et al., *Inorg. Chem.*, 2010, vol. 49, no. 6, p. 2901.
21. Fedushkin, I.L., Skatova, A.A., Yambulatov, D.S., et al., *Russ. Chem. Bull.*, 2015, vol. 64, p. 38.
22. Fedushkin, I.L., Lukoyanov, A.N., and Baranov, E.V., *Inorg. Chem.*, 2018, vol. 57, no. 8, p. 4301.
23. Fedushkin, I.L., Lukina, D.A., Skatova, A.A., et al., *Chem. Commun.*, 2018, vol. 54, no. 92, p. 12950.
24. Fedushkin, I.L., Lukoyanov, A.N., and Baranov, E.V., *Inorg. Chem.*, 2018, vol. 57, no. 8, p. 4301.
25. Lukina, D.A., Skatova, A.A., Lukoyanov, A.N., et al., *Dalton Trans.*, 2020, vol. 49, no. 9, p. 2941.
26. Lukina, D.A., Skatova, A.A., Sokolov, V.G., et al., *Dalton Trans.*, 2020, vol. 49, no. 41, p. 14445.
27. Sokolov, V.G., Lukina, D.A., Skatova, A.A., et al., *J. Struct. Chem.*, 2023, vol. 64, no. 9, p. 1724.
28. Fedushkin, I.L., Maslova, O.V., Morozov, A.G., et al., *Angew. Chem., Int. Ed. Engl.*, 2012, vol. 51, no. 42, p. 10584.
29. Bazyakina, N.L., Moskalev, M.V., Rumyantcev, R.V., et al., *Russ. Chem. Bull.*, 2023, vol. 72, p. 507.
30. Apostolidis, C., Deacon, G.B., Dornberger, E., et al., *Chem. Commun.*, 1997, no. 11, p. 1047.
31. Schumann, H., Heim, A., Demtschuk, J., et al., *Organometallics*, 2003, vol. 22, no. 1, p. 118.
32. Sulway, S.A., Layfield, R.A., Tuna, F., et al., *Chem. Commun.*, 2012, vol. 48, no. 10, p. 1508.
33. Lamberts, W. and Lueken, H., *Inorg. Chim. Acta*, 1987, vol. 132, no. 1, p. 119.
34. Evans, W.J., Rego, D.B., Ziller, J.W., et al., *Organometallics*, 2007, vol. 26, no. 19, p. 4737.
35. Sokolov, V.G., Lukina, D.A., Skatova, A.A., et al., *Russ. Chem. Bull.*, 2021, vol. 70, p. 2119.
36. Paulovicova, A.A., El-Ayaan, U., Shibayama, K., et al., *Eur. J. Inorg. Chem.*, 2001, vol. 2001, no. 10, p. 2641.
37. *Rigaku Oxford Diffraction (2021). CrysAlis Pro Software System, Version 1.171.41.122a*, Wroclaw: Rigaku Corporation.
38. Sheldrick, G.M., *Acta Crystallogr., Sect. A: Cryst. Adv.*, 2015, vol. 71, p. 3.
39. Sheldrick, G.M., *Acta Crystallogr., Sect. C: Struct. Chem.*, 2015, vol. 71, p. 3.
40. Spek, A.L., *Acta Crystallogr., Sect. C: Struct. Chem.*, 2015, vol. 71, p. 9.
41. Dodonov, V.A., Makarov, V.M., Zemnyukova, M.N., et al., *Organometallics*, 2023, vol. 42, no. 18, p. 2558.
42. Fedushkin, I.L., Skatova, A.A., Chudakova, V.A., et al., *Eur. J. Inorg. Chem.*, 2004, vol. 2004, no. 2, p. 388.
43. Skatova, A.A., Yambulatov, D.S., Fedyushkin, I.L., et al., *Russ. J. Coord. Chem.*, 2018, vol. 44, p. 400.
44. Long, J., Tolpygin, A.O., Cherkasov, A.V., et al., *Organometallics*, 2019, vol. 38, p. 748.
45. Woen, D.H., Kotyk, C.M., Mueller, T.J., et al., *Organometallics*, 2017, vol. 36, no. 23, p. 4558.
46. Janiak, C., *J. Chem. Soc., Dalton Trans.*, 2000, p. 3885.

Translated by E. Yablonskaya